A parametric study of a SOA based COEO for phase noise performance and reliable operation

Alexis Bougaud, Olivier Llopis, Arnaud Fernandez

A parametric study of a SOA based COEO for phase noise performance and reliable operation

Alexis Bougaud, Olivier Llopis, Arnaud Fernandez

***Abstract*—This paper presents experimental and numerical results on the effects of both intra and extra-cavity dispersion on a coupled opto-electronic oscillator (COEO) phase noise and its deterministic behavior. The combined effects of the optical intra-cavity dispersion and the detuning of the two oscillating loops strongly affects the COEO quality factor and its phase noise spectrum. The observed phase noise changes are correlated to the deterministic optical pulse shape, which turns out to be a simple parameter for noise optimization. The oscillation stability is also considered and particularly its dependence on the extra-cavity fiber spool dispersion. Finally, the dispersion management of a COEO can be completed by adjusting the Mach-Zehnder Modulator (MZM) bias voltage. By applying the proposed method, a phase noise performance below -120 dBc/Hz at 1 kHz offset from 10 GHz has been obtained.**

***Index Terms*—Coupled opto-electronic oscillator (COEO), phase noise, chromatic dispersion, detuning, mode-locked laser (MLL).**

I. INTRODUCTION

Conventional microwave and radio-frequency (RF) sources exploit surface or bulk acoustic wave resonance of quartz crystals. Quality factors (Q) of about 10^6 can be realized with this technology for a resonant frequency (f_{RF}) below 100 MHz and the oscillator signal is then multiplied up to the microwave range. The frequency multiplication process increases the phase noise floor and the signal must be filtered with a microwave oscillator locked to the quartz reference. High Q microwave sources have been developed to be used in such phase locked loops or for direct low phase noise generation at microwave frequencies, such as sapphire oscillators, but the Q factor of microwave resonators is inversely proportional to the f_{RF} value. It is thus impossible to get high Q in the upper range of microwave frequencies (millimeter wave range).

The Opto-Electronic Oscillator (OEO) [1,2] has been developed in order to take benefit of the low propagation losses typical in optical fibers. Indeed, a large time delay is equivalent to a very high Q factor and this Q is proportional to the f_{RF} value. Classical OEO is based on an opto-electronic feedback loop incorporating a few kilometers length optical delay-line, an externally modulated laser and a fast photodiode. However, a large fiber spool is detrimental for embedded systems as it reduces their compactness. It is also difficult to stabilize in temperature. Such fiber spool can be significantly reduced by using a resonator instead of the delay line and, finally, by incorporating the optical gain device inside the optical resonant loop, leading to the concept of the Coupled Opto-Electronic Oscillator (COEO) [1-3].

The COEO architecture is close to the Regenerative Mode-Locked Laser (RMLL). The oscillation is initiated by the spontaneous emission of the optical amplifier, feeding its own RF modulation signal after a photodetection located in the RF feedback loop (Fig.1). The optical and opto-electronic loops must be synchronized (both oscillators being coupled) and an RF resonator is used in the RF feedback to determine the optical pulse repetition rate. Such self-sustained oscillation favors the oscillator stability as any timing jitter experienced by one loop will be shared by the other after a cavity round trip. This represents one of the major benefits of a COEO compared to conventional external modulation systems (i.e. MLL).

This multidimensional system leads to complex dynamic in the optical domain and its impact on the RF signal is still difficult to interpret. Hence, the phase noise optimization of a COEO represent a challenging task requiring an accurate understanding of the relationship between the optical pulse properties and the resulting RF phase noise. To this aim, this paper will use the theorical framework proposed by A. Matsko in 2009 based on a gaussian assumption on the optical pulse shape [4], in order to generalize these results to any pulse shape obtainable by a fibered Semi-conductor Optical Amplifier (SOA) based COEO. We will specifically focus on two main parameters to optimize the COEO phase noise, namely: the chromatic dispersion and the frequency detuning between the two oscillators. A third parameter is used at the end of this paper: the DC voltage of the Mach Zehnder Modulator (MZM). Combining these parameters, a phase noise of -120 dBc/Hz at 1 kHz offset from 10 GHz has been obtained, both numerically and experimentally.

II. THE COEO-SOA BASED CONFIGURATION

The chromatic dispersion is one of the key experimental parameters which can be tuned to control the optical pulse shape and the RF phase noise [4,5]. This parameter will also impact the oscillator synchronization and affect the oscillator stability. As a result, the chromatic dispersion management need to be considered both for phase noise performance and oscillation

Manuscript received June 27, 2023.

This work was supported by the CNES (French National Center for Space Studies) and the Région Occitanie.

A. Bougaud, O. Llopis and A. Fernandez are with LAAS-CNRS, Université de Toulouse, CNRS, UPS, Toulouse, France (e-mail: bougaud@laas.fr, llopis@laas.fr, afernand@laas.fr). A. Bougaud is today at XLIM Limoges, France.

stability. The latter is mainly affected by the chosen COEO configuration. In our case, we focus on a SOA based COEO using a MZM, as depicted in Fig. 1. The SOA is a BOA1004P from Thorlabs based on a multi-quantum well structure, able to provide a small signal gain of more than 25 dB and a saturation power higher than 13 dBm. The SOA has been preferred to an EDFA for compactness considerations. A Chirped Fiber Bragg optical filter (CFBG) is also used to compensate the chromatic dispersion of the 400 m SMF fiber spool included in the optical loop. A second fiber spool is included in the COEO RF path for an easier synchronization between the optical and the opto-electronic loops. A high Q resonator at 10.29 GHz is also inserted in the RF feedback to select the RF harmonic of interest. The global RF losses are then compensated by two RF amplifiers providing respectively 26 dB and 10 dB gain. All optical elements are shared between the two oscillators here, excepted their respective delay-lines. The use of an SOA provides some degree of non-linearity inside the optical cavity, through the dynamic saturation of the gain and its slow recovery time. Thus, sharing the SOA between both loops minimizes its impact on the COEO synchronization, hence favoring stable oscillations. It is located before C_1 coupler, linking the MLL cavity to the OEO feedback, in order to improve the signal to noise ratio after photodetection. Finally, the COEO synchronization is changed using an RF variable delay-line represented as a phase shifter in Fig.1.

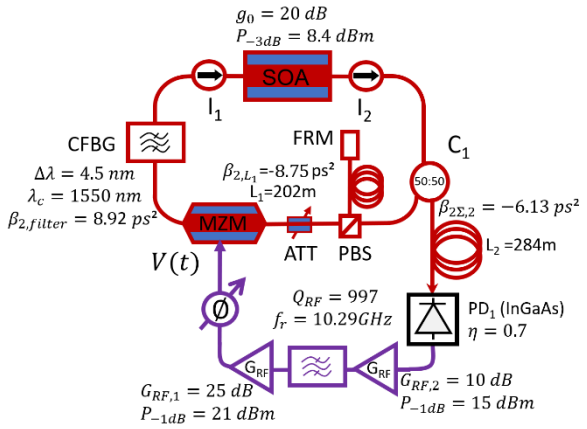

Fig. 1. Experimental COEO device. PD: photodiode, PBS: Polarization Beam Splitter, CFBG: Chirped Filter Bragg Grating, ATT: variable attenuator. $I_{1,2}$: optical isolator fast axis blocked. The intra-cavity dispersion is given by: $\beta_{2\Sigma,1} = \beta_{2,filter} + \beta_{2,L_1}$, when $\beta_{2\Sigma,2}$ is the extra-cavity dispersion. SOA: semi-conductor optical amplifier. MZM: Mach Zehnder Modulator.

In the last version of our system, the 400 m single path fiber spool in the optical cavity has been replaced by a 200 m two paths fiber ended by a Faraday mirror (FRM). Using this configuration together with a polarization beam splitter (PBS) allows not only a reduction in size but also a better control of the state of polarization (SOP) [6]. The linear SOP at the input of the SMF fiber spool is maintained at the output because the slow SOP changes perceived during the forward path are exactly compensated during the backward one. A variable optical attenuator is added at the output of this delay line to control the loop power. This configuration allows to control the SOP inside the optical loop without using a polarization maintaining (PM) fiber spool, the latter enhancing the phase noise because of polarization mode dispersion effect [7].

III. COEO NUMERICAL MODEL

A. *Theoretical framework and quality factor definition*

A. Matsko proposed an analytical approach based on the resolution of the master equation (1) [4,8]. The latter provides the temporal evolution of the slowly varying optical envelope. The pulse shape obtained at the steady-state is determined by different loop parameters such as the band-pass optical filter bandwidth Ω_f, the intra-cavity chromatic dispersion $\beta_{2\Sigma,1}$, the MZM function of modulation T_{MZM} and the SOA parameters (small signal gain g_0, gain recovery time τ_c, saturation power P_{sat} and the Henry factor α_h). Finally, the self-phase modulation induced by the Kerr effect in the fiber (γ_{NL}) are also considered.

$$T_R \frac{\partial A}{\partial T} = -\beta_1 \frac{\partial A}{\partial t} - \frac{i}{2}\left(\beta_{2\Sigma,1} + \frac{i}{\Omega_f^2}\right)\frac{\partial^2 A}{\partial t^2} + \left[\frac{1}{2}\left((1 - i\alpha_h)g(t) - \alpha\right) + T_{MZM}(u_{RF}) + i\gamma_{NL}|A|^2\right]A \quad (1)$$

$$\frac{\partial g}{\partial t} = \frac{g_0 - g}{\tau_c} - g\frac{|A|^2}{E_{sat}} \quad (2)$$

$$T_{MZM}(u_{RF}) = cos\left(\frac{\pi}{2V_\pi}(V_{bias} + u_{RF})\right) \quad (3)$$

At steady-state, the solution of this set of equations, leads to an optical pulse shape characterized by the pulse parameters $\{\xi, \Omega, q, \tau_p, E_p\}$, representing respectively the timing, carrier frequency, chirp, temporal width and energy of the optical pulse train. The timing can be related to the other parameters through the optical cavity components. For instance, the optical frequency comb carrier affects the pulse timing through the cavity chromatic dispersion ($\beta_{2\Sigma,1}$). The optical carrier itself can then be shifted in case of chirped pulses, by using the detuning between the optical pulse train and the MZM modulation signal (the detuning defined here as the frequency difference between the optical pulse train repetition rate and the RF signal frequency carried on the RF feedback loop: $\Delta f_{RF} = f_{OEO} - f_{MLL}$). The chirp also depends on the combined effect of chromatic dispersion, optical filtering losses (thus on the spectrum bandwidth) and SPM imposed by the SOA, so that all pulse parameters became related to each other and can be adjusted to impact the pulse train timing. This deterministic relationship can thus be exploited to reduce the pulse train timing jitter and as a result the RF timing one (t_m). Following Grein approximation [9], A. Matsko proposes to share this parameter space into two parts: the first set of variables $\{\xi, \Omega, t_m\}$ are used to study the synchronization process but also its impact on the COEO phase noise. This set became parametrized by the second one $\{q, \tau_p, E_p\}$ describing the optical pulse shape, so that the phase evolution of the RF and optical pulse train became closely related to the shape of individual pulses.

Considering this hypothesis, the RF and optical timing noise

sources are the two main contributors to the global RF phase noise. In addition, the optical carrier noise is converted into timing through second order chromatic dispersion (either intra or extra-cavity) or in case of chirped pulses [8-12]. Hence, the COEO phase noise will depend on its ability to damp the timing fluctuations $\delta\xi$ and the carrier fluctuations $\delta\Omega$ which can be related respectively to two quality factors: Q_+ and Q_-. The conversion mechanism of carrier fluctuation into timing one infers that both Q_+ and Q_- participate to the timing fluctuation damping and thus to the final quality factor of the COEO (Q_{COEO}). We can notice that these quality factors must be distinguished with Q_{MLL} and Q_{OEO} related to the ability of the MLL and the OEO to damp the RF timing fluctuation, independently on its noise source nature. In this way, $Q_\pm$ relate the COEO phase noise to the optical pulse parameters and are of particular interest for the experimenter intending to optimize the COEO phase noise by adapting the optical pulse shape.

On a first approximation, the Q_+ value is fixed by the timing constraint applied by the MZM, which is as important as the temporal pulse width regarding the temporal modulation window (blue curve in Fig. 2) and can be defined under gaussian assumption by: $Q_+ = 2T_R/(\Delta_{AM}\omega_m\tau_p^2)$, T_R being respectively the MLL round trip time, Δ_{AM} being the modulation depth [4]. The same way, Q_- represents the ability of the MLL to damp the optical carrier fluctuations and is given, under gaussian assumption, by: $Q_- = 2\omega_m T_R \tau_p^2 \Omega_f^2/(1+q^2)$. Taking into account that the optical spectrum width can be expressed by $\Delta\Omega_2^2 = (1+q^2)/\tau_p^2$, the ability of the MLL to damp the carrier fluctuations depends on the spectrum width and thus the filter bandwidth. In both cases, the increasing losses experienced by the optical pulses through the MZM and the band-pass filter reduce both quality factors of the MLL and depends on the pulse parameters $\{q, \tau_p, E_p\}$.

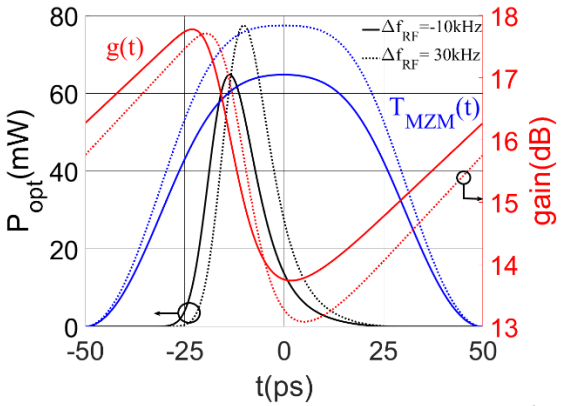

Fig. 2. Temporal pulse shape (black) simulated for $\beta_{2\Sigma,1} = -5\ ps^2$ for two detuning values: $\Delta f_{RF} = -10\ kHz$ (plain curves), $\Delta f_{RF} = 30\ kHz$ (dotted curves). The SOA dynamic gain (red) and the MZM modulation function (T_{MZM}(t) normalized to the optical pulse amplitude) are also presented and evolve with the pulse energy as the synchronization is improved. The time frame presented here is relative to the RF modulation timing.

The relationship between $Q_\pm$ and $\{q, \tau_p, E_p\}$, clearly identify how the deterministic behavior of the COEO through its optical pulse shape can be related to its phase noise performance. In this paper we will attempt to identify the effect of the COEO experimental parameters on the phase noise by changing optical pulse properties, and we will show how these parameters can be chosen in order to get at the same time low phase noise and stable oscillation. Among all experimental parameters, we will specifically focus on the impact of the chromatic dispersion $\beta_{2\Sigma,1}$ (intra-cavity) and $\beta_{2\Sigma,2}$ (extra-cavity).

The synchronization conditions being varied with the change of both dispersion values, the detuning between the opto-electronic loop and the optical one (Δf_{RF}) will also be considered in order to maintain stable oscillation and optimized phase noise conditions. We will then study how the MZM modulation signal can be adapted using its V_{bias} coupled to Δf_{RF} to optimize the COEO phase noise. By doing so, a phase noise of -120 dBc/Hz at 1kHz offset for an oscillation frequency of 10 GHz has been obtained experimentally as well as numerically, representing the lower phase noise measured so far with our SOA based COEO set-up (Fig.1).

B. Simulation of the deterministic COEO behavior

The COEO simulation was carried out through numerical integration of the MLL master equation (1) (alternative approach proposed in [13]). The solution obtained numerically provides the slowly varying pulse envelope before being detected by the photodiode feeding the RF chain included in the OEO. The resulting RF signal is then filtered by solving the second and first order differential equations of the high Q RF resonator and the low-pass filter of the photodiode respectively, considering periodic boundaries conditions. After amplification, the RF signal is then used as a parameter in the modulation function of the MZM $T_{MZM}(u_{RF})$ (eq.(2)). The short time scale is expressed in a frame relative to the maximum of the sinusoidal RF signal. The RF delay imposed by the RF phase shifter is considered here by applying a delay of opposite sign to the optical pulse train using β_1 coefficient, defined as: $\beta_1 = 2\pi\Delta f_{RF} T_R/\omega_m$ (with Δf_{RF} the frequency detuning between the optical pulse train and the modulation signal at the MZM location).

By using a semi-conductor amplifier (SOA), a dynamic saturation of the optical gain needs to be considered. The SOA instantaneous gain $g(t)$ is calculated solving eq. (2) parametrized by the SOA small signal gain ($g_0 = 20\ dB$), the 3 dB saturation power ($P_{sat} = 8.4\ dBm$) and the gain recovery time ($\tau_c \simeq 250\ ps$), for a current injection of 200 mA.
In addition, a Henry factor $\alpha_h = 3.5$ was chosen to consider the self-phase modulation experienced by the optical pulse train.
Regarding the shape of the optical filter, two cases were considered. The first one implements a gaussian shape and consider a chromatic dispersion limited to the second order. This way, the analytical tools developed by A. Matsko can be used to interpret the numerical results presented in this paper, affording a detailed control of the optical pulse shape based on experimental parameters. By doing so, we avoid the complexity inherent to our experimental set-up in our interpretation (complexity brought by the flat-top CFBG of Fig. 1, presenting non-negligible higher chromatic dispersion orders at its borders). We then show that even under such conditions, equivalent optical spectra can be obtained based on conventional experimental parameters adjustment. In the end of this paper, we will demonstrate the validity of our numerical

model and physical interpretations by comparing its results to experimental measurements.

C. COEO phase noise

The COEO noise results in the timing fluctuation of the optical pulse train. Based on Langevin approach [14], eq.(1) provides the diffusion coefficients of the optical field white noise in the optical cavity through the addition of a quantum Langevin Force: F. These fluctuations are related to quantum noise and estimated based on the fluctuation-dissipation theorem [14] relating the statistical photons emission and absorption to the average losses and gain experienced by the optical pulses. Based on eq.(4-5), Langevin forces for timing (F_ξ) and optical carrier (F_Ω) can be found using eq.(7-8) [8].

$$\frac{\mathrm{d}\xi}{\mathrm{d}T} = \int_{-\infty}^{\infty}(t-\xi)\left[A^*\frac{\partial A}{\partial T} + A\frac{\partial A^*}{\partial T}\right]dt + F_\xi \tag{4}$$

$$\frac{\mathrm{d}\Omega}{\mathrm{d}T} = -\frac{1}{E_p}\frac{dE_p}{dT}\Omega - \frac{i}{2E_p}\int_{-\infty}^{\infty}\left[\frac{\partial}{\partial T}\left(A^*\frac{\partial A}{\partial t}\right) - \frac{\partial}{\partial T}\left(A\frac{\partial A^*}{\partial t}\right)\right]dt + F_\Omega \tag{5}$$

$$t_m(\omega)e^{i\omega T_{oeo}} = \frac{\Delta_{RF}}{\Delta_{RF}+2i\omega}\left[\xi - \beta_{2\Sigma,2}\Omega + F_{shot}(\omega)\right] + F_{mw}(\omega) \tag{6}$$

$$F_\xi = \frac{1}{E_p}\int_{-\infty}^{\infty} t[A^*F + F^\dagger A]dt \tag{7}$$

$$F_\Omega = \frac{i}{E_p}\int_{\infty}^{\infty}\left[\frac{\partial A^*}{\partial t}F - F^\dagger\frac{\partial A}{\partial t}\right]dt \tag{8}$$

Equation (6) represents the RF timing evolution and complete the set of equations needed to study the COEO phase noise. Δ_{RF} represents the RF resonator FWHM, while F_{shot} and F_{mw} are the Langevin forces associated to the optical shot-noise and the RF noise. Flicker noise sources were added to the RF and optical white noise sources, accounting for the semiconductors components contributions to the optical and RF noise. To this purpose, the SOA and the RF amplifier flicker phase noise have been measured in an open loop configuration (residual phase noise measurement). Finally, this system of equations is used to study the pulse parameters fluctuations around their steady-state values [8-10].

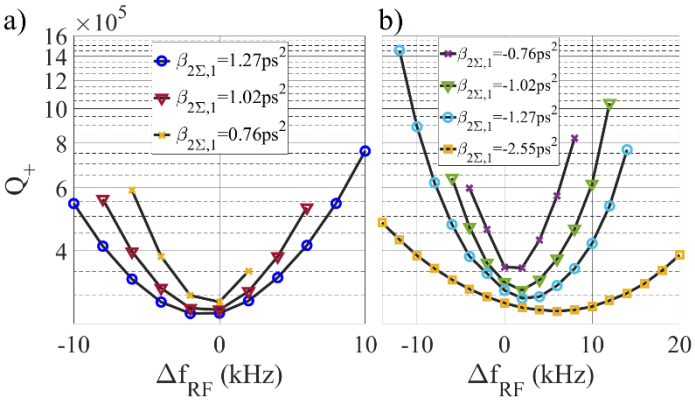

Fig. 3. Evolution of Q_+ over the COEO locking bandwidth for different intra-cavity dispersion (a- normal, b-anomalous, depicted for an equal y-scale) under gaussian filter assumption. The locking-bandwidth broaden as $|\beta_{2\Sigma,1}|$ increase.

Two of its eigenvalues provides the quality factors of the oscillators: $\{Q_+, Q_-\}$. The third one tends to zero as the RF phase of the COEO is kept free from any constraint. The COEO phase noise optimization is deeply related to the ability to control the optical pulse shape, which determines the COEO quality factors and the noise intensity [4]. The intra-cavity chromatic dispersion is, at this end, the experimental parameter impacting the most the optical spectrum. In the following sections, we will attempt to quantify its impact on the RF phase noise and to show how the COEO detuning needs to be managed in order to insure the oscillation stability.

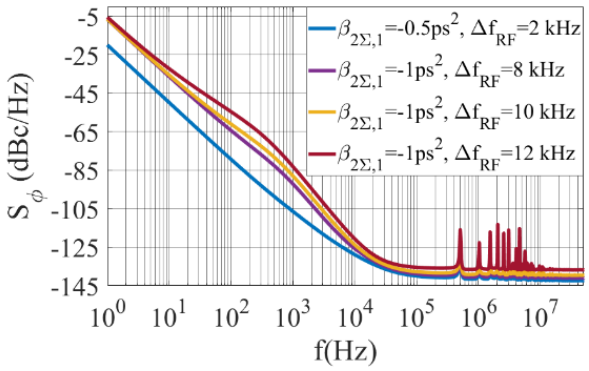

Fig. 4. Simulated phase noise evolution with detuning (Δf_{RF}) and for two intra-cavity chromatic dispersions: $\beta_{2\Sigma,1} = (-0.5, -1)\ ps^2$ under gaussian filter assumption.

IV. QUALITY FACTOR DEPENDENCE ON $\{\beta_{2\Sigma,1}, \Delta f_{RF}\}$

The COEO ability to damp its internal noise sources (F_ξ, F_Ω), can be estimated by its two quality factors ($Q_+$and Q_- respectively). Namely, the COEO capacity to damp timing fluctuations is deeply related to its ability to synchronize the RF signal and the optical pulse train. Therefore, we choose to study the COEO stability and its ability to damp its internal noise through the Q_+ factor, the latter being straightly related to the timing correction provided by the oscillator. The impact of detuning and intra-cavity chromatic dispersion on both stability and phase noise performance can then be considered at the same time through the COEO quality factor Q_+.

The timing constraint applied by the MZM on the optical pulse train and evaluated through Q_+, determine the coupling of the OEO towards the MLL: $C_{OEO\to MLL}$ (the optical coupler C_1 fixing the coupling ratio of the MLL towards the OEO: $C_{MLL\to OEO}$). The amount of coupling depends on the RF modulation power: a greater P_{RF} increase the coupling of the OEO towards the MLL, which in turn reduces the MLL quality factor. This effect can be visualized in Fig. 3, providing the evolution of Q_+ over the COEO locking bandwidth, for different $\beta_{2\Sigma,1}$ values. As the synchronization is improved, the modulation power increases (Fig.2), enhancing $C_{OEO\to MLL}$ and leading to a reduced quality factor for the MLL (Q_+). The lower Q_+ factors obtained, allows a significant oscillation stability enhancement by extending the instantaneous locking-bandwidth and making the oscillator lock more resilient to synchronization perturbations caused by noise sources. The opposite behavior is observed as the detuning get close to the borders of the bandwidth. It is to notice that this increasing quality factor at the locking borders is not necessarily related to a reduced phase noise, as it measures the COEO ability to filter timing fluctuations. The resulting phase noise also depends on the noise source intensity. Under high detuning values, the broader pulses obtained lead to a significant enhancement of the optical timing noise source [8] and thus decrease the global phase noise performance despite the high values of the quality factor obtained. Thus, the

synchronization conditions between OEO and MLL must be optimized to reduce the phase noise. This effect of synchronization on the RF phase noise can be observed in Fig. 4, when a significant phase noise reduction has been obtained on the intermediate frequency range ($f \in [10; 10^4]\ Hz$) as the synchronization of the COEO is improved.

As expected from mode-locking theory [15], the locking bandwidth displayed in Fig. 3 increases in average with $|\beta_{2\Sigma,1}|$ recalling that higher intra-cavity chromatic dispersions favor the oscillation stability. Moreover, the choice of the intra-cavity chromatic dispersion regime determines the range of Q_+ values obtainable. The higher Q_+ values observed under anomalous dispersion makes this configuration favorable for phase noise performance whereas the normal one favors the oscillation stability. To get both stability and phase noise performance, $\beta_{2\Sigma,2} > 0$ can be used under $\beta_{2\Sigma,1} < 0$ conditions, as detailed in section V.

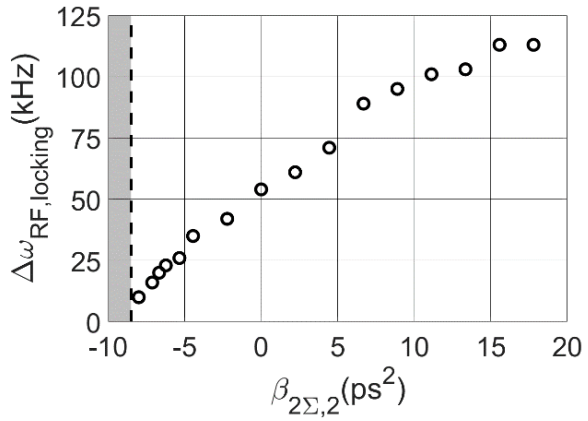

Fig. 5. Simulated locking-bandwidth evolution with $\beta_{2\Sigma,2}$ for $\beta_{2\Sigma,1} = -8.9\ ps^2$.The simulation was carried using the COEO parameters presented Fig.1 under gaussian filter assumption. No lock has been obtained for $\beta_{2\Sigma,2} < -10\ ps^2$, the end of the locking conditions being indicated by the black vertical dashed line.

V. Extra-cavity dispersion management: $\beta_{2\Sigma,2}$

The oscillation important parameters are stability and phase noise. This section presents a study aiming to determine an optimal extra-cavity dispersion allowing an enhanced oscillation stability, which can be coupled to the COEO phase noise performance obtained by adjusting $\beta_{2\Sigma,1}$ as explained in section IV.

The synchronization of the COEO depends on the differential delay between the two loops, which can be tuned thanks to the RF phase shifter. This differential delay defines the static detuning of the device but needs to be completed by the dynamic one, which results in the combination of chromatic dispersions of each spool $\{\beta_{2\Sigma,1}\ ,\ \beta_{2\Sigma,2}\}$ and the evolution of the optical carrier during the transient regime (Ω). In Fig. 4, the best phase noise is obtained both for low detuning and small intra cavity dispersion ($\beta_{2\Sigma,1} = -0.5\ ps^2$). A low intra-cavity chromatic dispersion is important for phase noise performance, but the COEO must keep its synchronization. The latter point is of major concern as a low intra-cavity chromatic dispersion reduces the COEO locking bandwidth (see Fig. 3). Indeed, the stability mainly depends on the dynamic delay due to the combined effect of chromatic dispersion and optical carrier frequency shift, given by:

$$\Delta t_{\Delta\beta_{2\Sigma}} = \Delta t_{\beta_{2\Sigma,1}} - \Delta t_{\beta_{2\Sigma,2}} = (\beta_{2\Sigma,1} - \beta_{2\Sigma,2})\Omega \qquad (9)$$

The dynamic feature of $\Delta t_{\Delta\beta_{2\Sigma}}$ lies in its dependence on Ω adjusted by the oscillator to maintain the MLL and the OEO locked together. Considering a synchronization perturbation, the required transient process towards locking conditions can lead to an important shift of the frequency comb carrier in case of low intra-cavity chromatic dispersion, thus increasing the loss imposed by the optical filter. This mechanism may make the locking conditions unreachable, leading to an unstable oscillation. As a result, $\Delta t_{\Delta\beta_{2\Sigma}}$ has to be minimized to insure a broad locking bandwidth. The dynamical delay required for synchronization, can then be obtained for a reduced carrier frequency shift Ω by choosing $\{\beta_{2\Sigma,1}, \beta_{2\Sigma,2}\}$ of opposite sign (eq. 9). To show the benefit of cumulative $\{\beta_{2\Sigma,1}, \beta_{2\Sigma,2}\}$ for the COEO stability, we numerically estimate the COEO locking-bandwidth evolution with $\beta_{2\Sigma,2}$, considering $\beta_{2\Sigma,1} = -8.9\ ps^2$ (i.e. without the CFBG chirp compensation). The result, presented in Fig. 5, shows a significant extension of the COEO locking bandwidth with the cumulative chromatic dispersion increase. High extra-cavity chromatic dispersion values, regarding the optical pulses chirp at the MLL output (out of C_1 coupler), will nevertheless lead to broaden pulses, enhancing the shot noise generated by the OEO's photodiode [16,17]. Thus, there is a trade-off between oscillation stability and phase noise performance. The $\beta_{2\Sigma,2}$ value for a specific $\beta_{2\Sigma,1}$, needs to be high enough to quench the optical carrier frequency shift still low enough to compensate the chirp adequately before photodetection. $\beta_{2\Sigma,1}$ affecting both the carrier frequency shift and the chirp, the two chromatic dispersions (intra and extra-cavity) need to be adjusted at the same time in order to satisfy both conditions.

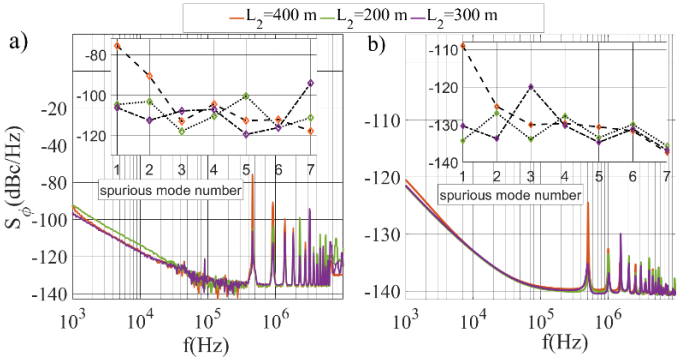

Fig. 6. Experimentally measured (a) and simulated (b) noise spurs amplitude for an intra-cavity fiber spool length $L_1 = 400\ m$ and an extra-cavity length L_2 so that $L_2/L_1 \in \{1, 1/2, 3/4\}$.

Finally, $\beta_{2\Sigma,2}$ being experimentally managed by adjusting L_2 (Fig.1), the choice of the extra-cavity chromatic dispersion has to be related to the one concerning the length of the OEO delay-line. Indeed, the noise spurs amplitude located at the frequency resonances shared by the MLL and the OEO, depends on the relative ratio of the two commensurable lengths L_2 and L_1. As $L_2 < L_1$ for a compact device, L_2 needs to be chosen to get a ratio L_2/L_1 close to a rational value n/m ($\{n, m\} \in \mathbb{N}^2$) with a denominator m as high as possible in order to minimize noise

correlation between OEO and MLL loops [18,19]. The noise spurs amplitude being maximized for the p^{th} harmonics for which $p.n/m \in \mathbb{N}$, increasing the denominator value allows to reduce the occurrence of maximal noise spurs amplitude, as depicted in Fig. 5. While a low close to carrier phase noise ($f < 1\ kHz$) is often the first parameter to be optimized, a reduced amplitude of the noise spurs is still of major importance for radar applications. Indeed, to make benefits of this low close to carrier phase noise, low noise spurs amplitude became necessary, as a signal weaker than the strongest noise spurs would be buried by the latter despite the low close to carrier phase noise. In our case, with a 400 m long optical cavity, the first spur is found at 500 kHz, as it can be seen in Fig. 6.

As a result, applying an extra and intra-cavity chromatic dispersion of opposite sign has to be favored for stable oscillation, keeping in mind that the ratio between extra and intra cavity fiber spool lengths has to be kept rational with the highest denominator possible in order to minimize the integrated timing jitter of the optical pulse train. This stability enhancement becomes particularly interesting in case of close to zero intra-cavity chromatic dispersion were the COEO stability is drastically reduced.

VI. Modulation Management Regarding the Chromatic Dispersion Regime

Beyond the only parameter of chromatic dispersion, it appears experimentally that the oscillator performance can be significantly enhanced by a fine adjustment of the modulation function of the MZM obtained by adjusting the MZM V_{bias} and detuning.

We first consider the case of a normal intra-cavity chromatic dispersion ($\beta_{2\Sigma,1} > 0$), with a $V_{bias} = V_\pi/2$ for the MZM. Under such conditions, the RF phase noise can be largely reduced by extending the optical spectrum through detuning.

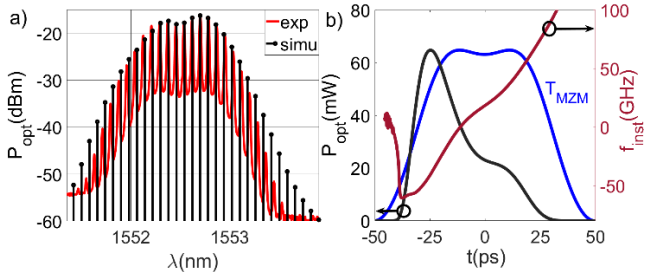

Fig. 7. a) Simulated optical spectrum based on a gaussian filter over a modulation period ($T_m = 100\ ps$, $\beta_{2\Sigma,1} = 10\ ps^2$) presenting a symmetric optical spectrum similar to experimental spectrum (red curve) the latter being obtained under conditions depicted in Fig.1. b) Simulated temporal pulse shape (black) and its instantaneous frequency (red) associated to the optical spectrum presented in a), synchronized to the MZM modulation window (blue).

The dynamical saturation of the SOA induces an asymmetric pulse, higher optical power being located at the leading edge. The positive chirp obtained relates this temporal asymmetry to the spectral one, so that the higher power spectral lines became located at the longer wavelengths of the optical spectrum. Hence, imposing a negative detuning ($\Delta f_{RF} < 0$) allows the experimenter to locate the related additional losses on the red side of the optical spectrum. By doing so, the instantaneous power on the leading edge is reduced just as the saturation level of the amplifier and the tailing edge of the optical pulse can take benefit of more available gain. This mechanism favors the blue side of the spectrum while attenuating the red one, leading a symmetrized spectrum (Fig. 7).

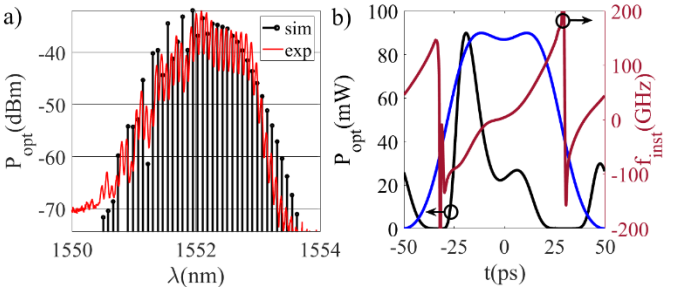

Fig. 8. a) Simulated optical spectrum based on a gaussian filter for $\beta_{2\Sigma,1} = 2.54\ ps^2$ and $V_{bias} = 0.7\ V_\pi$, compared to measurement (Fig.1). b) Temporal pulse shape associated to the optical spectrum simulated. The instantaneous frequency (red) source of the interferences on the spectrum blue side and the normalized MZM modulation signal (blue) are also indicated. The measured and simulation data were obtained with $G_{RF,2} = 26\ dB$ (Fig.1) to compensate the additional losses due to V_{bias}.

The spectral broadening obtained this way, leads to a significant reduction of the optical carrier noise contribution to the global phase noise. Indeed, in his analytical approach A. Matsko related the optical carrier contribution to the timing phase noise $S_\xi(\omega)$ by [9]:

$$S_\xi(\omega) = D_{\Omega\Omega}\frac{\tau_p^4\left(\beta_{2\Sigma,1}\Omega_f^2 - q\right)^2}{(1+q^2)^2} \qquad (10)$$

with $\Omega_f^2 = (1+q^2)/\tau_p^2$ being the optical spectrum width.

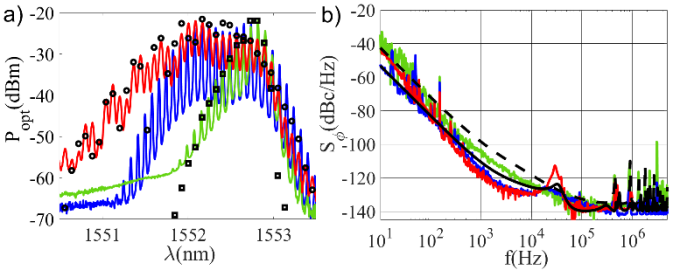

Fig. 9. a) Experimental spectra obtained for two different detuning values (green and blue). The blue spectrum is associated to a normal intra-cavity dispersion with a negatively detuned oscillator ($\Delta f_{RF} < 0$) for a MZM bias voltage $V_{bias} = V_\pi/2$ and leads to a significant phase noise reduction, and can be compared the green spectrum obtained for $\Delta f_{RF} = 0$. A broader spectrum (red curves) was obtained by changing the bias voltage ($V_{bias} = 0.7\ V_\pi$), improving the carrier phase noise contribution ($f \in [100\ Hz, 10\ kHz]$) presented in b). The simulated optical spectrum obtained under exact experimental parameters associated to red (black circles) and green (black squares) spectra (see Fig. 1 for simulation parameters details). Their respective simulated phase noises are presented by black curves in b) (red: continuous, green: dashed).

The optical carrier noise being predominant in the intermediate frequency range (i.e. $f \in [10^2; 10^4]\ Hz$), the experimental phase noise has been reduced by almost $10\ dB$ at $1\ kHz$ from the carrier compared to the usual red-shifted spectrum obtained without applying a negative RF detuning (green curves in Fig. 9). The spectrum extension can further be enhanced by increasing the MZM V_{bias} towards V_π. By doing so, the RF power favors odds harmonics (fundamental included) of the modulation signal frequency, thus spreading the energy over a

wider spectral range (Fig.8.a). The same approach was already used to favor the third harmonic generation of the oscillator [20]. A bias voltage close to the optical extinction value will also increase the static optical losses in the MLL, so that no oscillation can be realized with $V_{bias} \simeq V_{\pi}$. Hence, we choose a $V_{bias} = 0.7\, V_{\pi} = 3.9\, V$ in order to maintain an optical power level high enough to provide the opto-electronic loop gain necessary for the oscillation

Under such conditions, the MZM function imposes two modulation windows out of phase (Fig. 8.b), with a low extinction ratio. This causes the observed pulse doubling. Both pulses being positively chirped, identical instantaneous frequencies appear at two different time, making the shorter wavelengths to interfere. The broader spectrum obtained enhances the carrier phase noise reduction following eq. (10) and as it is clearly shown in Fig. 9 over the intermediate frequency interval ($f \in [100\ Hz, 10\ kHz]$), with a value of -120 dBc/Hz at 1 kHz offset from 10 GHz. The simulated phase noise and the associated optical spectrum (black curves) has been compared to the experimental ones (red and green curves) in Fig.9 and confirm our experimental observation.

VII. Conclusion

In this paper, a detailed modeling of a COEO has been presented. This model allows the simulation of the optical spectrum, the optical pulse properties and the RF phase noise versus the COEO parameters. It is used to investigate the COEO performance and stability versus the dispersion parameters of the two fiber spools: intra cavity and extra cavity spools. The detuning between the oscillators is also considered to get a stable oscillation. The simulated COEO Q factors increase near the zero intra cavity dispersion. However, this condition can be unstable as it is concomitant with a reduced locking bandwidth. The stability can then be enhanced by imposing an extra-cavity dispersion of opposite sign. These dispersion values are related to the fiber spool length of the opto-electronic and the optical loop, which need to be adjusted in order to reduce the phase noise spurs observed at high frequencies. Finally, a significant phase noise reduction can be obtained by adjusting the MZM V_{bias} and the detuning according to the intra-cavity chromatic dispersion. These conditions lead us to the best phase noise performance obtained with our set-up, i.e. -120 dBc/Hz at 1 kHz offset from the carrier. As a result, we recommend a low anomalous intra-cavity dispersion to favor phase-noise performance and a normal one in the secondary spool (RF path) for a stable oscillation.

References

[1] X. Yao and L. Maleki, “Dual microwave and optical oscillator”, Optics Letters, vol.22, no.24, pp.1867-1869, Dec. 1997.

[2] X.S. Yao, L. Maleki and D. Eliyahu, “Progress in the Opto-Electronic Oscillator a Ten Year Anniversary Review”, Int. Microwave Symposium (IMS) Digest, Fort Worth, USA June 2004

[3] D. Eliyahu and L. Maleki, “Modulation Respones (S_{21}) of the Coupled Opto-Electronic Oscillator”, Proc. of the Int. Freq. Control Symp. (IFCS), Vancouver, BC, Canada, August 2005.

[4] A. B. Matsko, D. Eliyahu, P. Koonath, D. Seidel, L. Maleki, “Theory of coupled optoelectonic microwave oscillator I: expectation values” *J. Opt. Soc. Am. B*, vol.26, no. 5, pp.1023-1031, May 2009.

[5] J. Davila-Rodriguez, K. Bagnell and P.J. Delfyett, “Frequency stability of a 10 GHz optical frequency comb from a semiconductor-based mode-locked laser with an intracavity 10,000 finesse etalon”, Optics Letters, vol.38, no.18, pp.3665-3668, September 2013.

[6] A. Liu, X. Li, S. Huo, T. Zhang, J. Dai and K. Xu “Polarization-insensitive coupled optoelectronic oscillator with low spurious tones and phase noise”, Optic Express, vol.30, no.6, pp.8700-8708, March 2022.

[7] A. Bougaud, A. Ly, G. Bailly, A. Fernandez and O. Llopis, “Effects of polarization mode dispersion on an all polarization maintaining fiber based coupled optoelectronics oscillators”, Proc. IEEE Int. Freq. Control Symp. (IFCS) and ISAF, Keystone, CO, USA, July 2020.

[8] A. B.Matsko, D. Eliyahu and L. Maleki “Theory of coupled optoelectronic microwave oscillator II: phase noise”, *J. Opt. Soc. Am. B*, vol.30, no.12, pp.3316-3323, Dec.2013.

[9] M. E. Grein, H. A. Haus, Y. Chen and E. P. Ippen, “Quantum-Limited Timing Jitter in Actively Modelocked Lasers”, *IEEE* Journal of Quantum Electronics, vol.40, no 10, pp.1458-1470, Oct. 2004.

[10] H. A. Haus, M. Margalit and C. X. Yu, “Quantum noise of a mode-locked laser”, J. Opt. Soc. Am. B, vol.17, no.7, pp.1240-1256, July 2000.

[11] F. Rana, R. J. Rajeev, and H. A. Haus, “Quantum Noise of Actively Mode-Locked Lasers With Dispersion and Amplitude/Phase Modulation”, Journal of Quantum Electronics, vol.40, no.1, pp.41-56, January 2004

[12] H. A. Haus, “Quantum Noise in Linear Amplifiers”, Phys.Rev. vol. 128, nº 5, pp.2407-2413, Dec.1962.

[13] L. Nielsen and M. J. R. Heck, “A computationally Efficient Integrated Coupled Opto-Electronic Oscillator Model”, Journal of Lightwave Technology, vol.38, no.19, pp.5430-5439, October 2020.

[14] M. Lax, “Classical Noise IV: Langevin Methods”, Reviews of Modern Physics, Vol.35, no.3, July 1966.

[15] O. P. McDuff and S. E. Harris, “Nonlinear Theory of the Internally Loss-Modulated Laser”, IEEE Journal of Quantum Electronics, vol.QE-3, no.3, pp.101-111, March 1967.

[16] F. Quinlan, T.M. Fortier, H. Jiang, A. Hati, C. Nelson, Y. Fu, J.C. Campbell and S.A. Diddams, “Exploiting shot noise correlation in the photodetection of ultrashort optical pulse trains”, Nature Photonics, vol.7, pp.290-293, April 2013.

[17] F. Quinlan, T.M. Fortier, H. Jiang and S.A. Diddams, “Analysis of shot noise in the detection of ultrashort optical pulse train”, J. Opt. Soc. Am. B, vol.30, no.6, pp.1775-1785, Jun 2013.

[18] F. Rana, H.L.T. Lee, R.J. Ram, M.E. Grein, L.A. Jiang, E.P. Ippen and H.A. Haus, “Characterization of the noise and correlations in harmonically mode-locked lasers”, J. Opt. Soc. Am. B, vol.19, no.11, pp. 2609-2621, Nov.2002.

[19] S. Gee, F. Quinlan, S. Ozharar and P. Delfyett, “Correlation of supermode noise of harmonically mode-locked lasers”, J. Opt. Am. B, vol.24, no.7, pp.1490-4597, July 2007.

[20] A. Ly, V. Auroux, R. Khayatzadeh, N. Gutierrez and A. Fernandez, “Highly Spectrally Pure 90-GHz Signal Synthesis Using a Coupled Optoelectronic Oscillator”, Photonics Technology Letters, vol.30, no.14, pp.1313-1316, July 2018.